Electron Spectroscopic Studies of Bis-(2,2′-bipyridine)-(4,4′-dicarboxy-2,2′-bipyridine)-ruthenium(II) and Bis-(2,2′-bipyridine)-(4,4′-dicarboxy-2,2′-bipyridine)-osmium(II) Adsorbed on Nanostructured TiO_2 and ZnO Surfaces

Karin Westermark,[†] Håkan Rensmo,[†] Anthea C. Lees,[‡,§] Johannes G. Vos,[§] and Hans Siegbahn*[,†]

Department of Physics, University of Uppsala, Box 530, S-751 21 Uppsala, Sweden, Department of Chemistry, Trinity College, Dublin 2, Ireland, and National Centre for Sensor Research, School of Chemical Sciences, Dublin City University, Dublin 9, Ireland

Received: November 15, 2001; In Final Form: May 23, 2002

The adsorption of the dyes bis-(2,2′-bipyridine)-(4,4′-dicarboxy-2,2′-bipyridine)-ruthenium(II) and bis-(2,2′-bipyridine)-(4,4′-dicarboxy-2,2′-bipyridine)-osmium(II) on nanostructured TiO_2 and ZnO was investigated by photoelectron spectroscopy (PES) using synchrotron radiation. Comparison of the results gives insight into the electronic structure of the molecules, as well as to their interaction with the substrates. The identity of the central metal ion of the dye complex was found not to influence the bonding mode of the molecule on the surfaces. However, when comparing the adsorption on the two metal oxides, the chemical state of the carboxyl group was found to be different. Binding to TiO_2 results in four chemically equivalent carboxyl oxygens, while the oxygens are found chemically nonequivalent for adsorption onto ZnO. In addition, information concerning the frontier electronic structure was obtained by measuring the valence band region by PES using different photon energies and the N1s near edge X-ray absorption spectroscopy (NEXAFS) spectra for the two molecules adsorbed on the surfaces.

Introduction

Dye-sensitized nanostructured film electrodes are intensively investigated today due to their potential use in solar cells.[1−3] The most efficient cells to date are based on ruthenium polypyridine complexes[4] having carboxylic acid groups attached to the nanocrystalline TiO_2 and ZnO surfaces.[5−12] Other sensitizing molecules have also been used[13−16] and among those osmium polypyridine complexes offer promise in developing high efficiency solar cells.

Dye-sensitized photoelectrochemical solar cells differ from conventional solar cells in that the function of light absorption is more clearly separated from the charge carrier transport for dye-sensitized solar cells. In these, a photocurrent is generated when a photon, absorbed by a dye molecule, induces electron injection into the conduction band of the semiconductor particle. In a regenerative solar cell, the dye must then be recycled by electron transfer from a redox species in the solution. The conversion efficiency therefore depends on the energy matching and a fast electron transfer between the sensitizing dye and the semiconductor as well as on such processes between the dye and the redox species. Hence, insight into the binding and electronic structure of these elements is important for the understanding and optimization of these cells.

Electron spectroscopy is a surface sensitive technique useful for studies of properties such as surface composition, adsorption geometries, distribution of energy levels and orbital symmetries.[17,18] As an example, the energy level matching between the highest occupied molecular orbital (HOMO) of the dye and the valence band of the semiconductor can be measured. These are in turn related to the positions of the energy levels of the excited dye and the conduction band, cf. Scheme 1.

SCHEME 1: The Relation between the Energy Diagram and the PES Spectrum for a Dye Molecule Adsorbed on a Semiconductor Surface[a]

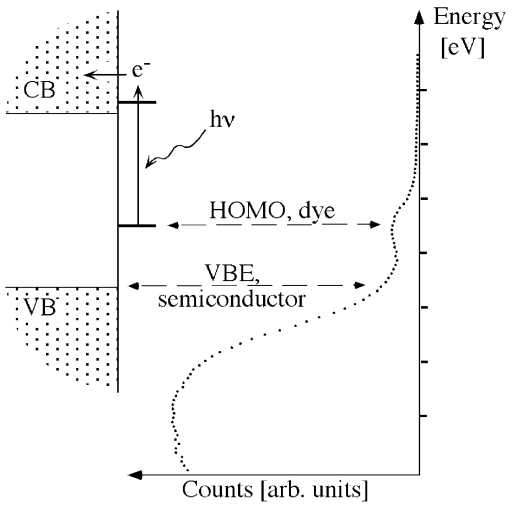

[a] The occupied energy levels (the valence band, VB, of the semiconductor and the highest occupied molecular orbital, HOMO, of the dye) are measured in the PES spectrum. The positions of the unoccupied levels can be related to those of the occupied energy levels via the band gap size of the semiconductor and the optical absorption spectra of the dye.

* To whom correspondence should be addressed. E-mail: hans.siegbahn@fysik.uu.se.
[†] University of Uppsala.
[‡] Trinity College.
[§] Dublin City University.

10.1021/jp014218z CCC: $22.00
Published on Web 09/07/2002

In this study electron spectroscopy is used to compare two different metal polypyridine complexes attached to nanostructured oxide surfaces. Specifically, bis-(2,2′-bipyridine)-(4,4′-dicarboxy-2,2′-bipyridine)ruthenium(II) (RuL_2L') and bis-(2,2′-bipyridine)-(4,4′-dicarboxy-2,2′-bipyridine)osmium(II) (OsL_2L') adsorbed onto nanostructured TiO_2 and ZnO films were investigated.

Experimental Section

The preparation of the nanostructured films is described in ref 5. The TiO_2 films used here were 2 μm thick with a nanoparticle size of 10 nm (Ti-nanoxide T, purchased from Solaronix S. A., Aubonne, Switzerland), and the ZnO films were 10 μm thick with a nanoparticle size of 150 nm.[19]

The synthetic procedure of the dyes [bis-(2,2′-bipyridine)-(4,4′-dicarboxy-2,2′-bipyridine)ruthenium(II)]$^{2+}\cdot 2PF_6^-$ (RuL_2L') and [bis-(2,2′-bipyridine)-(4,4′-dicarboxy-2,2′-bipyridine)osmium-(II)]$^{2+}\cdot 2PF_6^-$ (OsL_2L') is described in refs 20 and 21. The sensitization processes were carried out in a way similar to those used for efficient solar cells.[5] The TiO_2 and ZnO films were sintered at 450 °C, allowed to cool to about 80 °C and then soaked in 0.5 mM ethanolic solutions of the dye for 8 and 0.5 h, respectively. For the dyes used in the present study these preparations are expected to represent close to monolayer coverage. This was found by comparing relative peak intensities of the dye and the metal oxide substrate in the valence regions with results from earlier investigations.[17,18] In a comparison between $Ru(L')_2(NCS)_2$ and the dyes used here, it may be mentioned that $Ru(L')_2(NCS)_2$, having four carboxyl and two thiocyanate units, formed Zn^{2+}/dye aggregates more readily, as determined by visual inspection of the front and backside of heavily sensitized nanostructured films. For a ZnO electrode sensitized for a long time with the $RuL'_2(NCS)_2$ dye, the electrode was strongly colored on the solution side, while it remained uncolored on the opposite, glass-substrate side. The RuL_2L'- and OsL_2L'-sensitized electrodes were, on the other hand, evenly colored throughout the films.

Photoelectron spectra were obtained using synchrotron radiation at beamline I411 of the Swedish National Synchrotron Source MAX-lab.[22] All spectra are energy calibrated vs the N1s peak of the dyes (set to E_B = 400.0 eV [17]). NEXAFS measurements were performed by recording the secondary electrons with the electron spectrometer (SCIENTA, SES-200), and were calibrated using first- and second-order light.

The frontier orbital structure for the RuL_3 molecule, tris-(2,2′-bipyridine)-ruthenium(II), with different different Ru−N bonding distances (the bipyridine molecular structure was the same) was calculated using a semiemperical quantum chemical model (ZINDO).[23−29]

Results and Discussion

O1s. Carboxyl groups are commonly used for anchoring of dyes on metal oxide surfaces. For molecules of the kind studied here, both monodentate ester type, having nonequivalent oxygens, and bidentate bridge type, having equivalent oxygens, have been proposed when anchoring TiO_2 (schematically shown in Scheme 2).[38−42]

Information of the bonding interaction and geometry of carboxylated molecules can be obtained from the O1s photoelectron spectra. For a nonbonded molecule, the O1s spectrum contains two peaks originating from the two different oxygens (−OH and =O) in the carboxyl group.[30,31] In contrast, measurements of submonolayers of formic acid and 4,4′-dicarboxy-2,2′-bipyridine (the L′ ligand) adsorbed onto a TiO_2 surface display a single peak for the carboxyl oxygens indicating that the carboxyl groups are deprotonated, i.e., all oxygens bind to surface Ti ions, and become chemically equivalent. In these studies[30−32] a bridge bonding mode was found. For formic acid and L′ molecules adsorbed onto rutile TiO_2 (110), the position of the peak of the binding oxygen is very close to the position of the doubly bonded O1s peak in the nonbonded molecule, and is shifted about 1.6 eV toward higher binding energies from the position of the TiO_2 substrate peak.[30,32]

The O1s spectra for RuL_2L' and OsL_2L' adsorbed on nanostructured TiO_2 and ZnO are shown in Figure 1. The results for TiO_2 (1a,b) are very similar to those obtained for the surface-adsorbed carboxylated molecules discussed above, i.e., the spectra contain two peaks: one peak originating from the TiO_2 and one peak, shifted about 1.6 eV toward higher binding energies, originating from the oxygens in the carboxyl groups. As discussed above, this indicates a bridge bonding structure

SCHEME 2: Common Binding Modes of Carboxylic Acids on Metal Oxide Surfaces[a]

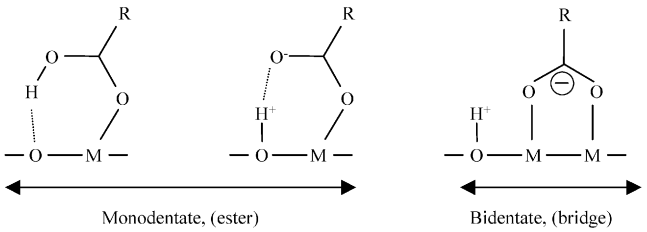

[a] The experimental results strongly indicate the bidentate binding for adsorption onto TiO_2. For adsorption onto ZnO nonequivalent oxygens are measured indicating a monodentate binding mode.

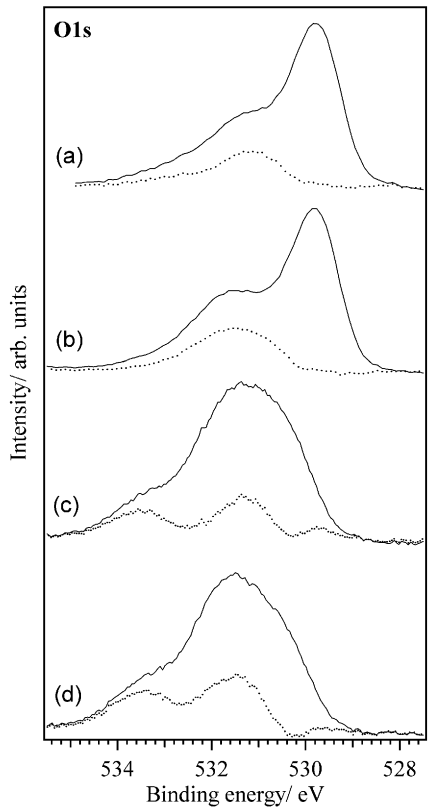

Figure 1. O1s core level spectra (lines) of (a) OsL_2L' on TiO_2 (b) RuL_2L' on TiO_2 (c) OsL_2L' on ZnO, and (d) RuL_2L'on ZnO ($h\nu$ 758 eV). The dotted lines under each spectrum show the difference spectra obtained after subtracting the corresponding O1s substrate signal (measured for a plain film and intensity normalized versus the bulk substrate peak) from each spectrum.

involving all four carboxyl oxygens, in a fashion where all oxygens are deprotonated (COO^-). Such a structure is also supported by theoretical calculations.[17,43−44]

The match between the geometries of the oxide surface and the adsorbing molecule has a decisive influence on the possible interactions between a larger molecule and a substrate. Therefore, geometrical differences between the oxides studied here, such as the metal−metal distance (TiO_2 3.8 Å, ZnO 3.2 Å) may be important for the possibilities to form strong bonds. Theoretical work on formic acid adsorbed on ZnO suggests, however, that both monodentate and bidentate bonding are possible.[44,45]

The O1s spectra measured for RuL_2L' and OsL_2L' adsorbed onto nanostructured ZnO are shown in Figure 1c,d. The RuL_2L'- and OsL_2L'-sensitized surfaces display almost identical O1s spectra having a peak at about 531.4 eV and shoulders at 533.4 and 530.4 eV. Comparing these spectra with the O1s spectrum measured for unsensitized ZnO, the major difference observed is an increased intensity at higher binding energy (533.4 eV), which is close to the position where the protonated oxygens in multilayers of nonbonded carboxyl groups normally appear. Therefore, comparing with the TiO_2 case, the O1s spectra measured for the dye molecules adsorbed onto ZnO display a difference in the chemical state for the linking units. The binding energy shifts suggest a bonding geometry containing nonequivalent oxygens similar to the nonbonded dye molecule. In this bonding mode (monodentate) the geometrical positions and the interactions involving the hydrogen span a large number of possibilities (see Scheme 2). However, our binding energy data indicates at least a substantial interaction between the hydrogen and the carboxyl group of the dye molecular adsorbate. Such bonding geometries have been proposed based on calculations.[33,34] These calculations also suggest that other configurations may be favorable and that mixtures (depending on surface coverage) may form.

C1s. Interpretations of C1s spectra always suffer from the contributions of the carbon contamination present in sample preparations of this kind. However, shifts and intensities measured for the carboxyl groups were earlier observed to follow trends expected from surface linking via the carboxyl group, showing only small effects due to hydrocarbon contamination for similar preparations to the ones in this study.[17]

Figure 2a shows the C1s spectra of the RuL_2L'-sensitized nanostructured TiO_2 (the peak at 281 eV is $Ru3d_{5/2}$). The C1s spectra of the RuL_2L'- and OsL_2L'-sensitized nanostructured TiO_2 and ZnO films are very similar in that they contain a major C1s peak at 285 eV and a minor peak at higher binding energy originating from the carboxyl group. The position of the carboxyl C1s peak (see Figure 2b) is the same for both the RuL_2L' and the OsL_2L' dye when binding to TiO_2, and the peak is shifted toward lower binding energies compared to nonbonded carboxyl groups.[17] This result is therefore in line with deprotonation of the binding carboxyl groups.

When adsorbing onto ZnO, the position of the carboxyl group C1s peak is the same for the two complexes. Interestingly, however, comparing the two substrates (TiO_2 and ZnO) the carboxyl C1s peak shifts toward higher binding energies when binding to ZnO. These results are in line with the O1s results above and support the conclusion that the chemical state for the carboxyl group is different when binding to ZnO compared to TiO_2.

Ru3d and Os4f. The $Ru3d_{5/2}$ peak measured for the Ru dye adsorbed onto ZnO and TiO_2 is shown in Figure 3. Both spectra contain a single peak (fwhm 0.8 eV) having the same binding energy, as expected for a pure dye. For the RuL_2L' adsorbed onto TiO_2, the binding energy relative to Ti3p is the same as that measured for similar compounds having one and six carboxyl groups.[17]

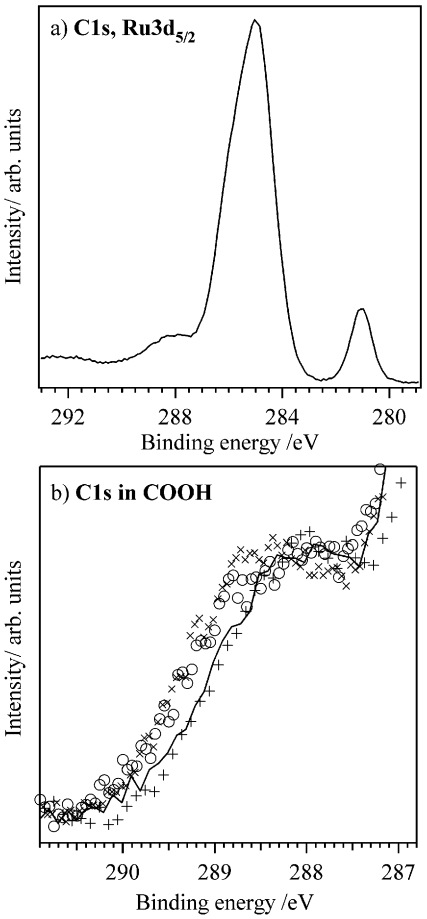

Figure 2. C1s core level spectrum of RuL_2L' on TiO_2 ($h\nu$ 758 eV). The inset shows an expansion of the region around the carboxyl C1s signal for OsL_2L' on TiO_2 (+), RuL_2L' on TiO_2 (line), OsL_2L' on ZnO (), and RuL_2L' on ZnO (×).

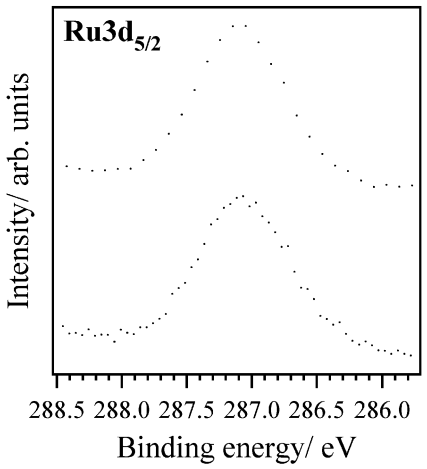

Figure 3. $Ru3d_{5/2}$ core level spectra of RuL_2L' on TiO_2 (top) and ZnO (bottom) ($h\nu$ 397 eV).

The $Os4f_{5/2}$ and $Os4f_{7/2}$ peaks measured for the Os dye adsorbed onto ZnO and TiO_2 are shown in Figure 4. As for the Ru3d peaks, the positions of the Os4f peaks are very similar for the two substrates. The peaks can be fitted with single Voigt profiles (fwhm 1.0 eV). Thus also the osmium complex was found to be pure with no contamination by complexes with other ligands.

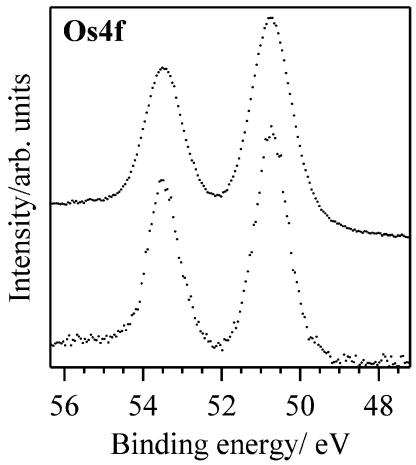

Figure 4. Os4f core level spectra of RuL_2L' on TiO_2 (top), and ZnO (bottom) resolved into its spin−orbit components ($h\nu$ 454 eV).

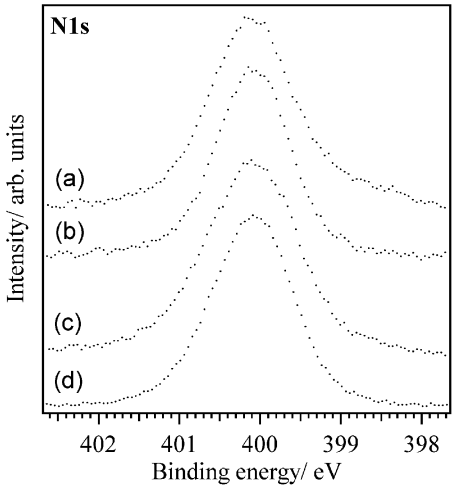

Figure 5. N1s core level spectra of (a) OsL_2L' on TiO_2, (b) RuL_2L' on TiO_2, (c) OsL_2L' on ZnO, and (d) RuL_2L' on ZnO ($h\nu$ 758 eV).

N1s. The N1s spectra for RuL_2L' and OsL_2L' adsorbed onto TiO_2 and ZnO are shown in Figure 5. All six nitrogens in the adsorbed RuL_2L' and OsL_2L' complexes are chemically equivalent, and it is therefore to be expected that a single N1s peak is obtained in all four cases. This is in accordance with the experimental results, as seen in Figure 5. More interesting, however, is that the N1s binding energy relative to the substrate peaks is the same for the OsL_2L' and RuL_2L' complexes. This was found both when adsorbing the dyes onto nanostructured TiO_2 (N1s relative to Ti2p) and when adsorbing the dyes onto ZnO (N1s relative to Zn3d). This result shows that the coordinating nitrogens are in very similar chemical states, and accordingly, the donation of electrons to the central metal atom is closely the same in all cases.

Valence Level Spectra. Figure 6 shows the valence level spectra of sensitized nanostructured TiO_2 and ZnO films recorded at a photon energy of 758 eV. In all spectra the occupied outermost orbitals of the OsL_2L' and RuL_2L' complexes are clearly distinguished above the valence band edge of the semiconductor (cf. Scheme 1). In Figure 7, the valence level spectra measured at different photon energies are shown. The substantial variations in the intensity of the highest occupied molecular orbital, HOMO, compared to the valence band, are well accounted for by differences in photoelectric cross sections. The intensity minimum at 150 eV is expected when the HOMO level of the complex has a dominating Ru4d or Os5d character.[17,34]

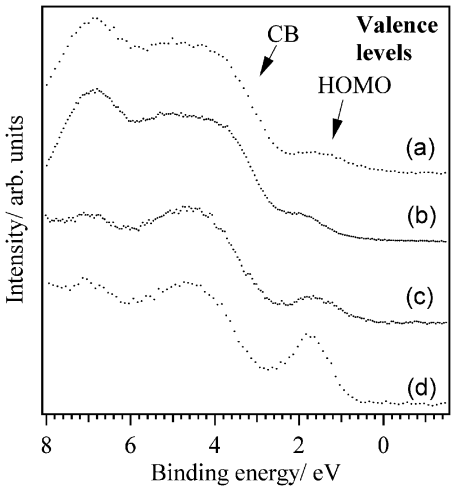

Figure 6. Valence level spectra of (a) OsL_2L' on TiO_2, (b) RuL_2L' on TiO_2, (c) OsL_2L' on ZnO, and (d) RuL_2L' on ZnO ($h\nu$ 758 eV). The highest occupied molecular orbital, HOMO, is clearly distinguished above the valence band, VB, of the metal oxides.

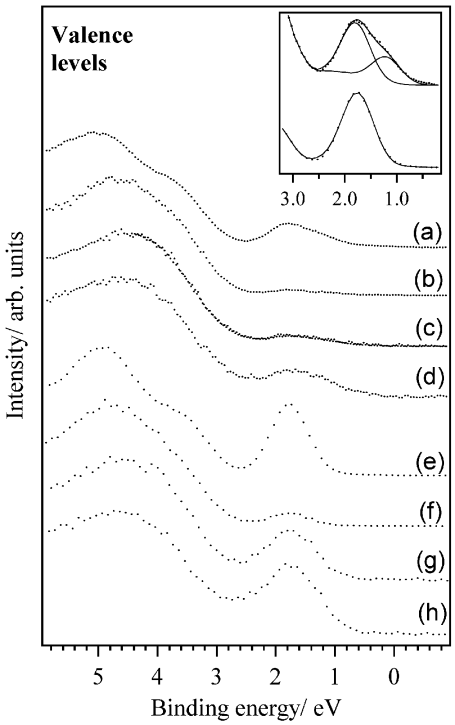

Figure 7. Valence level spectra of (a)−(d) OsL_2L' and (e)−(h) RuL_2L' on ZnO measured at different photon energies: (a,e) 60 eV, (b,f) 150 eV, (c,g) 454 eV, and (d,h) 758 eV. The inset shows curve fits of the frontier orbital structure of the OsL_2L' on ZnO (top) and RuL_2L' on ZnO (bottom) measured at 60 eV.

For complexes having comparable solvent interactions one would expect a correlation between the oxidation potential and the position of the HOMO level. Solvent interactions (and other intermolecular interactions) depend on geometrical structures and overall molecular charge distributions. One would therefore expect the HOMO of OsL_2L' to have a lower binding energy than the HOMO of RuL_2L', since the geometrical structures and overall charge distribution are very similar for the two complexes, and since OsL_2L' has a lower redox potential (OsII/OsIII is at 0.81 V vs SCE) than that of the RuL_2L' (RuII/RuIII is at 1.23 V vs SCE).[13] In view of this, it might seem surprising that the peak positions are similar in all cases (see Figure 7). A detailed analysis of the spectra shows, however, that the HOMO

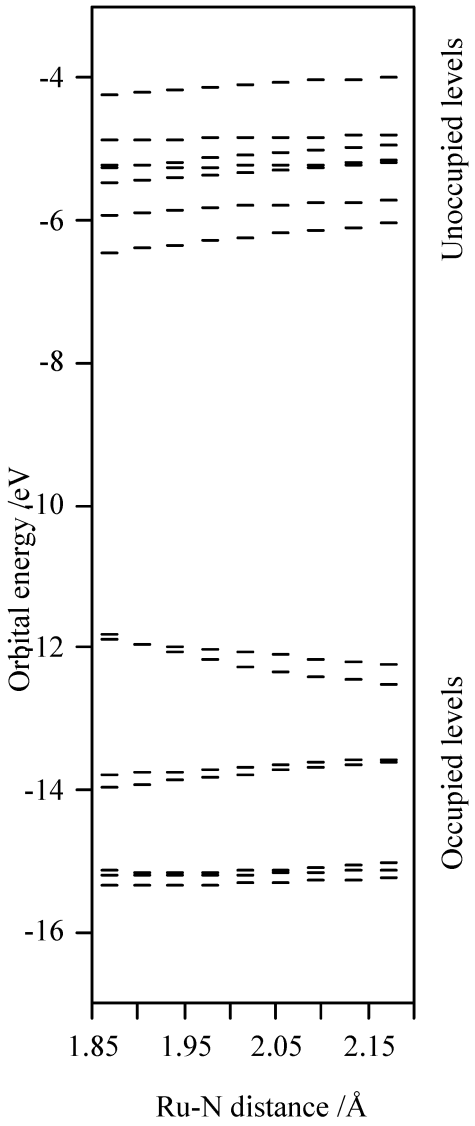

Figure 8. The frontier orbital structure for the RuL_3 molecule, tris-(2,2′-bipyridine)-ruthenium(II), with different geometries (different Ru−N bonding distances, the bipyridine molecular structure is the same) calculated using a semiemperical quantum chemical model (ZINDO). The two energy levels at about −12 eV consist of the doubly degenerate energy level (the e_g set) and the singly degenerate energy level (a_1).

level is broader for OsL_2L' compared to RuL_2L'. This difference is most clearly seen in the spectrum of the sensitized ZnO measured at a photon energy of 60 eV (Figure 7, inset). In this case, the HOMO level for RuL_2L' can be fitted with a single Gaussian with a fwhm of 0.71 eV, while it is clearly asymmetric for OsL_2L'. This asymmetric peak can be deconvoluted with two Gaussians, having a fwhm of 0.65 eV with an intensity ratio of 2:1 and separated by 0.6 eV. One explanation to this asymmetry could be the presence of impurities in the osmium complex. This is, however, unlikely since the spin−orbit coupled Os4f peaks can be fitted with single Voigt profiles as described above.

Instead, a possible explanation for this difference between the Ru and the Os complex is as follows: The frontier orbital structure of OsL_2L' and RuL_2L' is often interpreted within an octahedral symmetry in which the HOMO contains three degenerate orbitals (the t_{2g} set). The true symmetry of the complexes is however lower (D_3), which splits the three HOMO levels into the doubly degenerate energy level (the e_g set) and the singly degenerate energy level (a_1). The magnitude of this

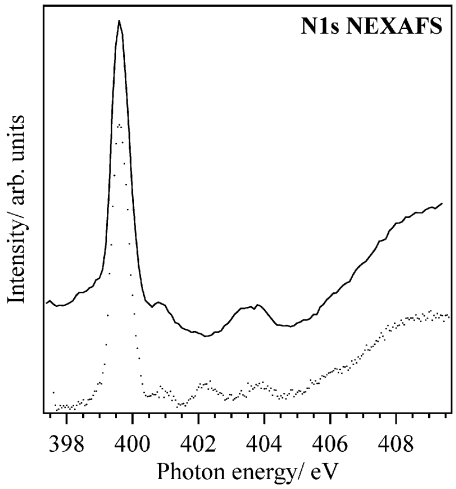

Figure 9. N1s NEXAFS spectra of OsL_2L' (top, line) and RuL_2L' (bottom, dots) on TiO_2.

splitting depends on the geometry (i.e., the orbital overlap) and the difference in energy between interacting orbitals on the metal center and the ligands. This dependence is displayed in Figure 8, showing the frontier orbital structure for the RuL_3 molecule with different geometries (different Ru−N bonding distances) obtained from semiempirical (ZINDO, refs 23−29) calculations. Thus, while a Ru−N and Os−N bonding distance of 2.056 Å (equal to the true crystal structures[35,36]) results in a small binding energy difference between the e_g and a_1 orbitals (0.23 eV) for RuL_2L', a different behavior may be expected for OsL_2L'. This is due to differences in the extension of the Ru4d and Os5d orbitals as well as in their orbital energies. The deconvolution of the asymmetric peak for OsL_2L' into two peaks having a ratio of 2:1 is therefore in accordance with an orbital picture in which the splitting in the e_g and a_1 levels is large enough to be resolved in the spectra. The position of the proposed single HOMO level (a_1) is shifted about 0.6 eV with respect to the peaks measured for the RuL_2L' complex, a value comparable to the difference in redox potential of 0.42 V measured for the two complexes.

NEXAFS Spectra. Differences in the frontier orbital structure also affect the electronic excitations within the molecule. For example, the difference in binding energy of the HOMO discussed above is in accordance with the measured shift in the optical absorption spectra[13] assuming that the positions of the lowest unoccupied states for the two complexes are the same.

In a NEXAFS measurement, unoccupied valence states are probed by excitation of core electrons to these levels. In this study, the unoccupied levels containing nitrogen are probed by excitation of N1s electrons. The lowest unoccupied states for these molecules are generally expected to be ligand centered. Since the N1s binding energies with respect to the substrate peaks are found to be the same for both dye complexes, a direct comparison of the unoccupied level structure of the complexes can be made.

The NEXAFS spectra for the dyes adsorbed on TiO_2 are shown in Figure 9. As can be seen, the first two resonances (reflecting the electronic structure of the lowest unoccupied states) are very similar in energy position, shape, and relative intensities, whereas there are some differences in the higher resonances.

To understand the NEXAFS spectra of the complexes, a comparison with that of the L′ ligand is useful. In ref 37, the NEXAFS spectra for the L′ ligand is measured and compared with a calculated counterpart. The first, main, resonance appears

at about 1 eV lower photon energy for L′ than for the present metal complexes.[30,37] In a first approximation, this can be understood as an effect of the introduction of a doubly charged central ion complexing to the nitrogens. This will lead to a lowering in the electronic energy levels, resulting in higher binding energies of the N1s level. This effect will lead to a shift upward in energy of the NEXAFS spectrum (thus appearing at higher photon energies), since the N1s core level shifts more than the valence levels.

The presence of a central ion will also lead to a general shift of electron density toward the nitrogen atom region. This polarization effect will result in a general appearance of new peaks in the spectrum, since unoccupied orbitals will gain density on the nitrogens. This effect may be quite sensitive to the character of the central ion, thus resulting in intensity gains which are different for the two complexes studied here. A difference between the complexes is observed, as seen in Figure 9, in that the third resonance is absent or shifted toward higher photon energies in the OsL_2L' case.

Conclusions

OsL_2L' and RuL_2L' adsorbed on nanostructured ZnO, and TiO_2 have been investigated by photoelectron spectroscopy (PES) and near edge X-ray spectroscopy (NEXAFS). The molecular configuration of the two molecules was found to be different when adsorbed onto the two metal oxides. The O1s spectra obtained for the molecules binding to TiO_2 support the view that all four carboxyl oxygens bind in the same way (probably in a bridge bonding mode). For the dyes adsorbed onto ZnO, on the other hand, the O1s spectra are clearly different, indicating monodentate bonding with a substantial interaction between the hydrogen and the carboxyl group of the dye molecular adsorbate.

The identity of the central metal ion in the dye complex does not seem to influence the bonding mode of the molecule. Furthermore, the donation of electrons from the ligands to the metal center was found to be similar for both dye complexes, as seen by the lack of shift in the N1s binding energy for the different dyes.

A detailed investigation of the valence region shows that the occupied frontier orbital structure differs between the two complexes. Thus, comparing the structure to that expected for octahedral complexes, the lowered symmetry (D_3) splits the t_{2g} energy level; a splitting found to be larger for the Os complex than for the Ru analogue. Differences between the complexes were observed also in the unoccupied valence levels, as seen in the N1s NEXAFS spectra.

Acknowledgment. This work was supported by the European Training and Mobility of Researchers Program (TMR), Grant CT96-0076; the Swedish Research Council (VR); and the Foundation for Strategic Research, Sweden (SSF). Dr. Karin Keis is gratefully acknowledged for supplying us with the ZnO films.

References and Notes

(1) O'Regan, B.; Grätzel, M. *Nature* **1991**, *353*, 737.
(2) Hagfeldt, A.; Grätzel, M. *Chem. Rev.* **1995**, *95*, 49.
(3) Hagfeldt, A.; Grätzel, M. *Acc. Chem. Res.* **2000**, *33*, 269.
(4) Gerfin, T.; Grätzel, M.; Walder, L. *Prog. Inorg. Chem.* **1997**, *44*, 345.
(5) Nazeeruddin, M. K.; Kay, A.; Rodicio, I.; Humphrey-Baker, R.; Müller, E.; Liska, P.; Vlachopoulos, N.; Grätzel, M. *J. Am. Chem. Soc.* **1993**, *115*, 6382.
(6) O'Regan, B.; Moser, J.; Anderson, M.; Grätzel, M. *J. Phys. Chem.* **1990**, *94*, 8720.
(7) Kalyanasundaram, K.; Nazeeruddin, M. K.; Grätzel, M.; Viscardi, G.; Savarino, P.; Barni, E. *Inorg. Chim. Acta* **1992**, 20.
(8) Argazzi, R.; Bignozzi, C. A.; Heimer, T. A.; Castellano, F. N.; Meyer, G. J. *Inorg. Chem.* **1994**, *33*, 5741.
(9) Hagfeldt, A.; Didriksson, B.; Palmqvist, T.; Lindström, H.; Södergren, S.; Rensmo, H.; Lindquist, S.-E. *Sol. Energy Mater. Sol. Cells* **1994**, *31*, 481.
(10) Cao, F.; Oskam, G.; Searson, P. C. *J. Phys. Chem.* **1995**, *99*, 17071.
(11) Knödler, R.; Sopka, J.; Harbach, F.; Guenling, H. W. *Sol. Energy Mater. Sol. Cells* **1993**, *30*, 277.
(12) Rensmo, H.; Keis, K.; Lindström, H.; Södergren, S.; Solbrand, A.; Hagfeldt, A.; Lindquist, S.-E.; Wang, L. N.; Muhammed, M. *J. Phys. Chem. B* **1997**, *101*, 2598.
(13) Sauvé, G.; Cass, M. E.; Coia, G.; Doig, S. J.; Lauermann, I.; Pomykal, K. E.; Lewis, N. S. *J. Phys. Chem. B* **2000**, *104*, 6821.
(14) Sauvé, G.; Cass, M. E.; Doig, S. J.; Lauermann, I.; Pomykal, K.; Lewis, N. S. *J. Phys. Chem. B* **2000**, *104*, 3488.
(15) Alebbi, M.; Bignozzi, C. A.; Heimer, T. A.; Hasselmann, G. M.; Meyer, G. J. *J. Phys. Chem. B* **1998**, *102*, 7577.
(16) Farzad, F.; Thompson, D. W.; Kelly, C. A.; Meyer, G. J. *J. Am. Chem. Soc.* **1999**, *121*, 5577.
(17) Rensmo, H.; Westermark, K.; Södergren, S.; Kohle, O.; Persson, P.; Lunell, S.; Siegbahn, H. *J. Chem. Phys.* **1999**, *111*, 2744.
(18) Rensmo, H.; Södergren, S.; Patthey, L.; Westermark, K.; Vayssieres, L.; Kohle, O.; Brühwiler, P. A.; Hagfeldt, A.; Siegbahn, H. *Chem. Phys. Lett.* **1997**, *274*, 51.
(19) Keis, K.; Vayssières, L.; Rensmo, H.; Lindquist, S.-E.; Hagfeldt, A. *J. Electrochem. Soc.* **2001**, *148*, A149.
(20) Shimidzu, T.; Iyoda, T.; Izaki, K. *J. Phys. Chem.* **1985**, *89*, 642.
(21) Lees, A. C.; Evrard, B.; Keyes, T. E.; Vos, J. G.; Kleverlaan, C. J.; Alebbi, M.; Bignozzi, C. A. *Eur. J. Inorg. Chem.* **1999**, *12*, 2309.
(22) Bässler, M.; Forsell, J. O.; Björneholm, O.; Feifel, R.; Jurvansuu, M.; Aksela, S.; Sundin, S.; Sörensen, S. L.; Nyholm, R.; Ausmees, A.; Svensson, S. *J. Electron Spectrosc. Relat. Phenom.* **1999**, *103*, 953.
(23) Zerner, M. C. *Reviews in Computational Chemistry*; VCH Publishers: New York, 1991; Vol. 2.
(24) Zerner, M. C.; Loew, G. H.; Kirchner, R. F.; Müller-Westerhoff, U. T. *J. Am. Chem. Soc.* **1980**, *102*, 589.
(25) Ridley, J.; Zerner, M. *Theor. Chim. Acta* **1973**, *32*, 111.
(26) Bacon, A. D.; Zerner, M. C. *Theor. Chim. Acta* **1979**, *53*, 21.
(27) ZINDO, Version 1988. The ZINDO program package was developed by M. Zerner and co-workers, University of Florida, Gainesville, Florida; ZINDO, Ed.
(28) For the parameters, the default values set by the program were used ($f_{\sigma\sigma'} = 1.267$ and $f_{\pi\pi'} = 0.585$ and for ruthenium $\beta(5s) = \beta(5p) = -2.0$ and $\beta(4d) = -32.0$).
(29) Rensmo, H.; Lunell, S.; Siegbahn, H. *J. Photochem. Photobiol. A* **1998**, *114*, 117−124.
(30) Patthey, L.; Rensmo, H.; Persson, P.; Westermark, K.; Vayssières, L.; Stashans, A.; Petersson, Å.; Brühwiler, P. A.; Siegbahn, H.; Lunell, S.; Mårtensson, N. *J. Chem. Phys.* **1999**, *110*, 5913.
(31) Westermark, K.; Rensmo, H.; Siegbahn, H.; Keis, K.; Hagfeldt, A.; Ojamäe, L.; Persson, P. *J. Phys. Chem. B* **2002**, *106*, 10102.
(32) Chambers, S. A.; Thevuthasan, S.; Kim, Y. J.; Herman, G. S.; Wang, Z.; Tober, E.; Ynzunza, R.; Morais, J. *Chem. Phys. Lett.* **1997**, *267*, 51.
(33) Persson, P.; Lunell, S.; Ojamäe, L. *Surf. Sci.* Submitted for publication.
(34) Yeh, J. J.; Lindau, I. *At. Data Nucl. Data Tables* **1985**, *32*, 1.
(35) Rillema, D. P.; Jones, D. S.; Levy, H. A. *J. Chem. Soc., Chem. Commun.* **1979**, *19*, 849.
(36) Richter, M. M.; Scott, B.; Brewer, K. J.; Willett, R. D. *Acta Crystallogr.* **1991**, *C47*, 2443.
(37) Persson, P.; Lunell, S.; Brühwiler, P. A.; Schnadt, J.; Södergren, S.; O'Shea, J. N.; Karis, O.; Siegbahn, H.; Mårtensson, N.; Bässler, M.; Patthey, L. *J. Chem. Phys.* **2000**, *112*, 3945.
(38) Meyer, T. J.; Meyer, G. J.; Pfennig, B. W.; Schoonover, J. R.; Timpson, C. J.; Wall, J. F.; Kobusch, C.; Chen, X. H. Peek, B. M.; Wall, C. G.; Ou, W.; Erickson, B. W.; Bignozzi, C. A. *Inorg. Chem.* **1994**, *33*, 3952.
(39) Murakoshi, K.; Kano, G.; Wada, Y.; Yanagida, S.; Miyazaki, H.; Matsumoto, M.; Murasawa, S. *J. Electroanal. Chem.* **1995**, *396*, 27.
(40) Vinodgopal, K.; Hua, X.; Dahlgren, R. L.; Lappin, A. G. ;Patterson, L. K. Kamat, P. V. *J. Phys. Chem.* **1995**, *99*, 10883.
(41) Duffy, N. W.; Dobson, K. D.; Gordon, K. C.; Robinson, B. H. ;McQuillan, A. J. *Chem. Phys. Lett.* **1997**, *266*, 451.
(42) Finnie, K. S.; Bartlett, J. R.; Woolfrey, J. L. *Langmuir* **1998**, *14*, 2744.
(43) Persson, P.; Lunell, S. *Sol. Energy Mater. Sol. Cells* **2000**, *63*, 139.
(44) Persson, P.; Stashans, A.; Bergström, R.; Lunell, S. *Int. J. Quantum Chem.* **1998**, *70*, 1055.
(45) Nakatsuji, H.; Yoshimoto, M; Umemura, Y; Takagi, S.; Masahiko, H. *J. Phys. Chem.* **1996**, *100*, 694.